A SEMI-AUTOMATIC METHOD TO SEGMENT MULTIPLE SCLEROSIS LESIONS ON FLAIR MAGNETIC RESONANCE IMAGES

L. Storelli[1], P. Preziosa[1,2], E. Pagani[1], V. Martinelli[2], G. Comi[2], A. Falini[3], M. Filippi[1,2], M.A. Rocca[1,2]

[1]Neuroimaging Research Unit, [2]Department of Neurology, [3]Department of Neuroradiology, Institute of Experimental Neurology, Division of Neuroscience, San Raffaele Scientific Institute, Vita-Salute San Raffaele University, Milan, Italy.

INTRODUCTION and PURPOSE

The analysis of disease burden using MR images from patients with multiple sclerosis (MS) requires the quantification of the volume of hyperintense lesions on a T2-weighted MRI sequence.[1] Several automatic methods for MS lesion segmentation on FLAIR MR sequences have been proposed, that benefit from CSF signal suppression and better contrast between focal lesions and the surrounding tissue.[2] However, due to the high rate of false positive and false negative lesions identified, manual segmentation is still the gold standard.

Aim of this study is to adapt and validate on FLAIR MR images a semi-automatic method recently developed for MS lesion segmentation on (DE) PD/T2-weighted MRI scans.[3,4]

METHODS

MRI Acquisition: FLAIR MRI scans (TR/TE = 8000/90 ms; flip angle = 90°) were acquired on a 1.5T Philips Achieva scanner from 17 patients with clinically isolated syndrome (CIS) suggestive of MS (mean lesion load=2.5 ± 2.3 ml).

Methods: The core of the algorithm remained the pixel-based region growing segmentation method: this approach examines neighbouring pixels of initial "seed points" and determines whether the pixel neighbours should be added to the segmented region according to similarity constraints. The expansion of the segmented region continued to the adjacent pixels until the stop condition was reached for all neighbouring pixels [1]:

$$Stop\ condition = \underbrace{I_i > Th_i}_{(1)} \cap \underbrace{I_i \notin F_{edges}}_{(2)}; \quad [1]$$

1) The first constraint examined whether the intensity of the new pixel I_i was smaller than a computed threshold Th_i [2]:

$$\left. \begin{array}{l} Th_i = I_{seed_i} - w_i * G_i; \\ G_i = 0.25 * I_{seed_i}; \end{array} \right\} \quad Th_i = I_{seed_i} * (1 - 0.25 * w_i); \quad [2]$$

Where I_{seed_i} was the image intensity of the $i\text{-}th$ seed point. The intensity gradient (**Gi**) was expressed considering that lesions are outliers on FLAIR histogram. Thus, defining the 75th percentile of the histogram as cut-off for the outliers (**Figure 1**), a new pixel cannot be segmented as lesion (outlier) if its intensity is smaller than the 25% of the maximum intensity. Since I_{seed_i} not always represents the maximum intensity on the FLAIR histogram, we introduced a weight coefficient (w_i) to correct for lesions heterogeneity.
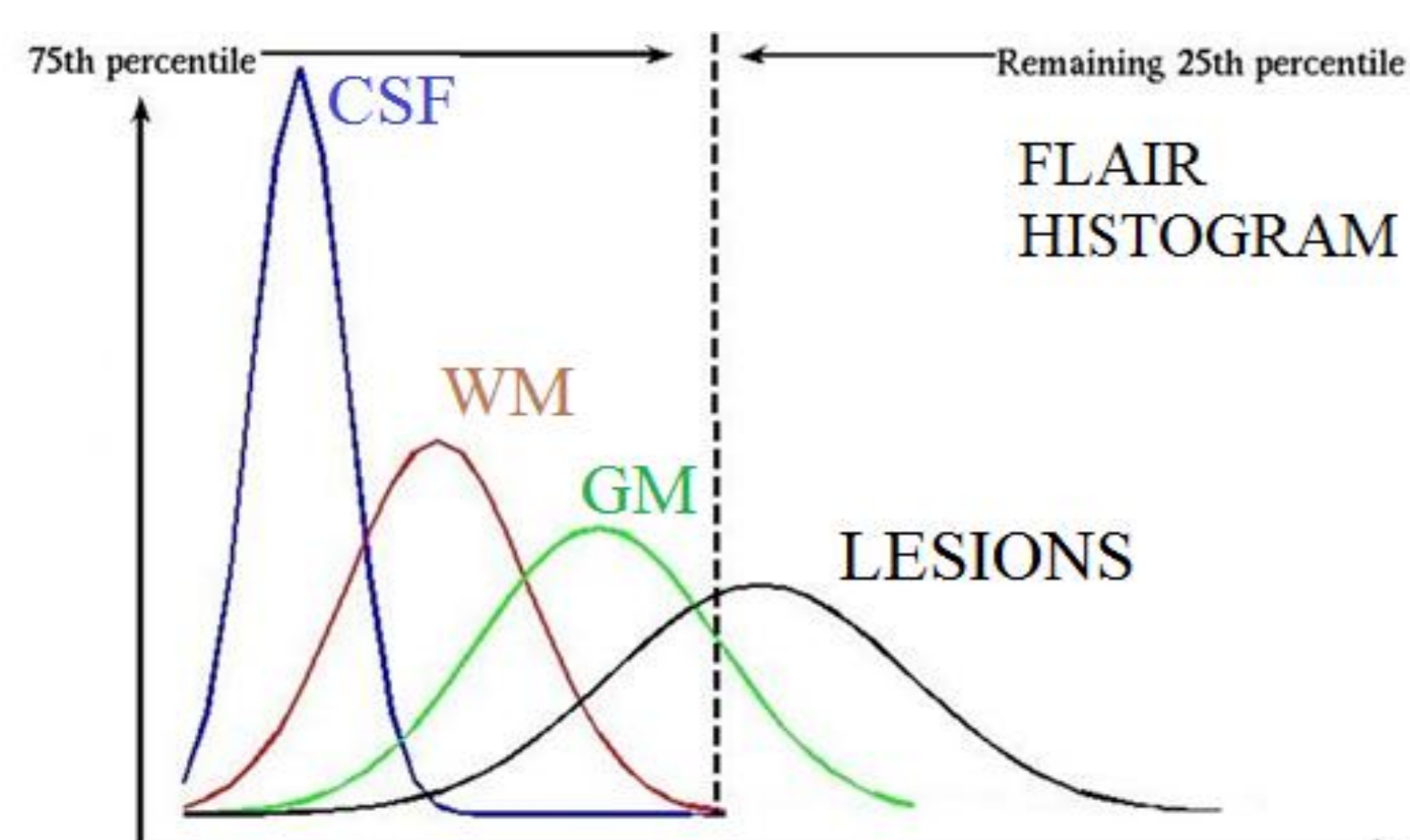

Figure 1. A schematic example of a FLAIR MRI histogram. The lesions could be considered as outlier intensities, since they exceed the 75th percentile of the histogram.

2) The second constraint for the stop condition examined whether the $i\text{-}th$ pixel I_i exceeded lesion edges (F_{edges}), found by high-pass filtering the FLAIR image. The metrics evaluated were Dice Similarity Coefficient (DSC), Root Mean Squared Error (RMSE) of lesion load, True Positive Fraction (TPF), False Positive Fraction (FPF), and False Negative Fraction (FNF) for each patient.

RESULTS

The validation measures averaged over all patients were obtained: DSC = 64%; TPF = 0.8; FPF = 0.32; FNF = 0.19 (**Figure 2**); RMSE = 0.65 ml.
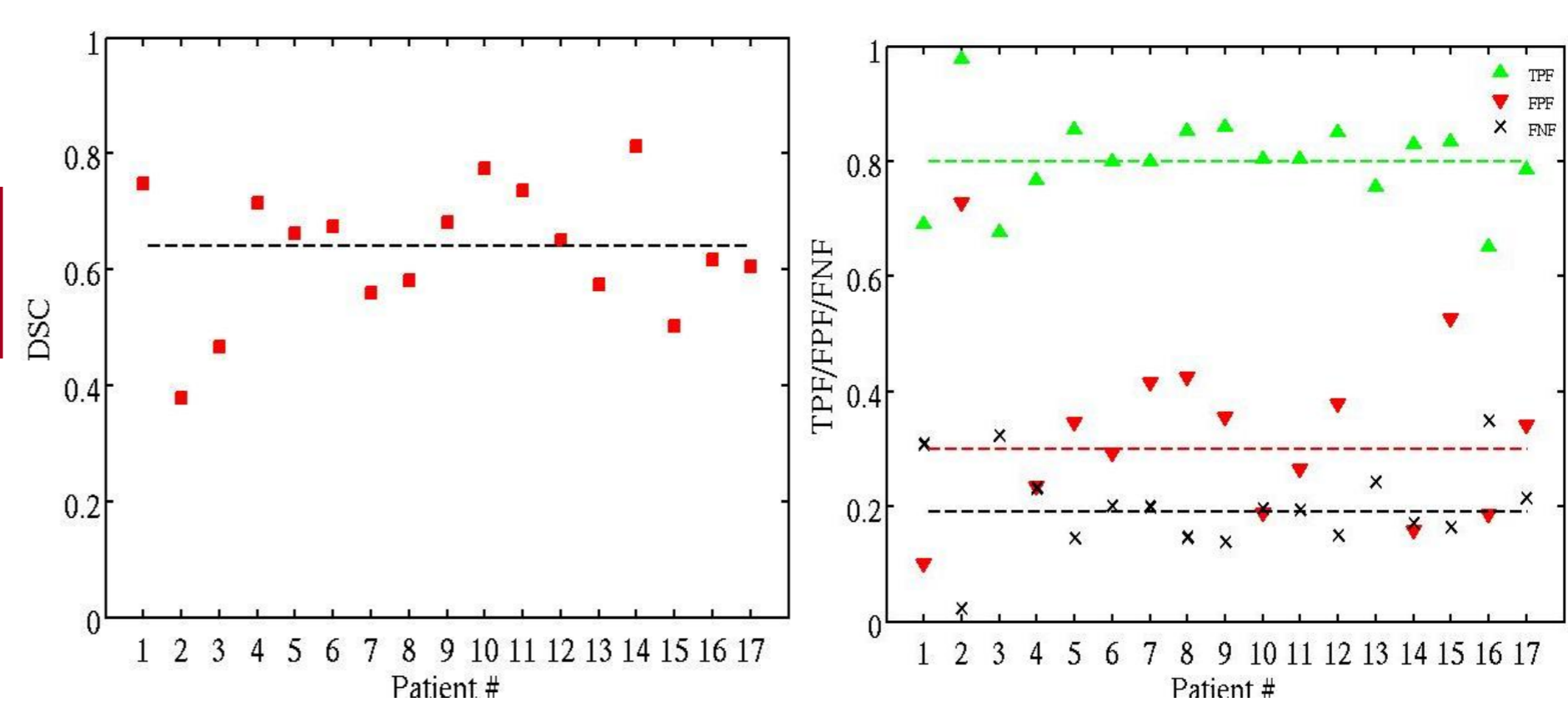

Figure 2. DSC values for all patients are reported in the left graph; while TPF, FPF and FNF values are shown in the right graph.

Figure 3. Examples of lesion segmentation for two different patients (in the two rows) performed by the proposed method (in red) compared to the gold standard (manual segmentation) (in blue). The corresponding FLAIR images are shown in the right column.
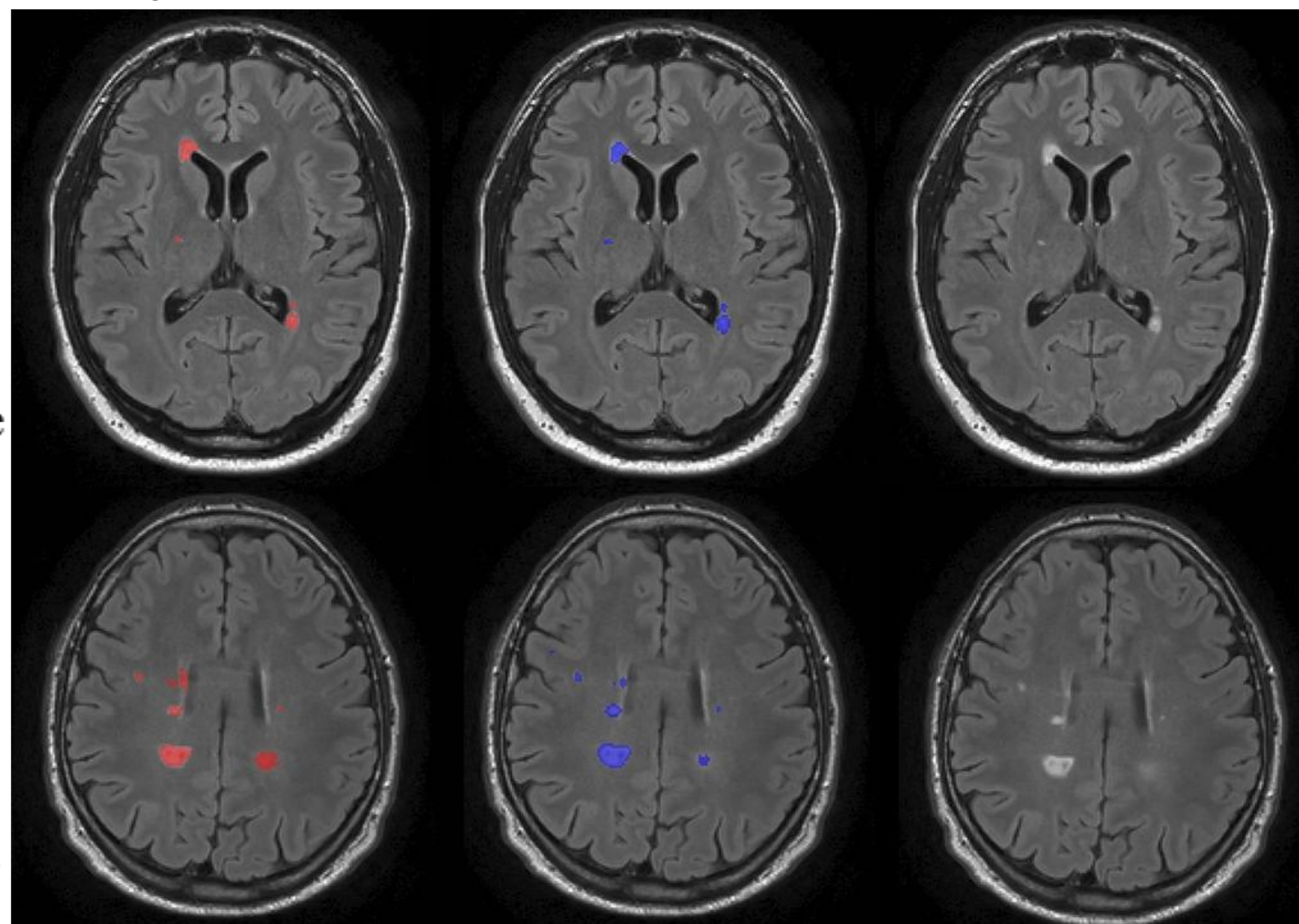
CONCLUSIONS

- **Using this method, lesion segmentation is very similar to manual segmentation and no center-specific training is required.**
- **It prevents the false positive and false negative lesion detection through the manual identification.**
- **With the automatic lesion contouring, lower operator time will be required for image analysis using the proposed method.**

REFERENCES

[1] Filippi et al., Arch Neurol 2011; [2] Garcia-Lorenzo et al., Med Image Anal 2013; [3] Storelli et al., BrainLes, MICCAI 2015; [4] Storelli et al., AJNR 2016.